Supplementary Information - Shaping Exciton Dynamics in 2D Semiconductors by Tailored Ultrafast Pulses

Omri Meron[1,2†], Uri Arieli[1,2†], Eyal Bahar[1,2], Swarup Deb[1], Moshe Ben-Shalom[1] and Haim Suchowski[1,2]

[1]Condensed Matter Physics Department, School of Physics and Astronomy, Faculty of Exact Sciences , Tel Aviv University, Tel-Aviv, 6997801, Israel.
[2]Center for Light-Matter Interaction, Tel Aviv University, Tel-Aviv, 6997801, Israel.

Contributing authors: omrimeron@tauex.tau.ac.il; uriarieli14@gmail.com;
[†]These authors contributed equally to this work.

Note A Single-pulse four wave-mixing

The interaction between Ultrafast broadband lasers with a nonlinear mediator enables the generation of various intrapulse wave-mixing processes, as illustrated in Fig. A1. The four-wave mixing (FWM) signal refers to the nonlinear signal arising from three frequency components which sum generates a forth frequency component within, but also in the outskirts of the generating pulse bandwidth. To obtain a background-free signal we usually truncate the high-frequency portion of the broadband pulse and detect the so-called 'Anti-Stokes' FWM signal that forms near the pulse edge. Such a third-order nonlinear signal is advantageous over other nonlinear spectroscopic techniques for not being limited by symmetry constraints, by improved spatial scanning resolution, and by a relatively simple experimental setup. FWM has mainly been utilized for single pulse coherent anti-Stokes Raman scattering (CARS) [1, 2], nonlinear coherent spectroscopy for label-free detection [3] as well as other applications [4].

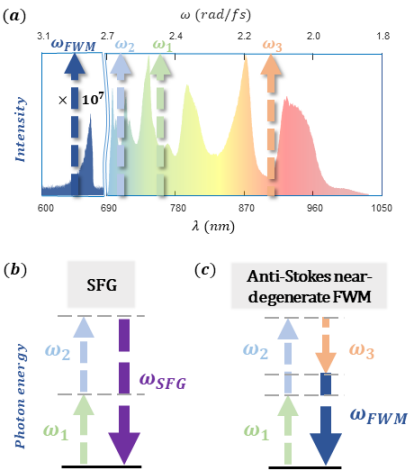

Fig. A1 Single-pulse ultrafast nonlinear wave-mixing processes. (a) Right: our ultrabroad-band laser distribution in the frequency domain ($690-1030nm$). Left: The nonlinear Anti-Stokes near-degenerate four-wave mixing (FWM) spectrum ($600-690nm$). (b-c) Schematic illustration of two selected wave-mixing process of superimposed photons from our ultra-broadband pulse (the arrows are colored in correspondence with the laser spectrum from (a)). (b) Sum frequency generation (SFG). (c) Anti-Stokes near-degenerate FWM.

Note B Single-pulse resonant Sum Frequency Generation (SFG)

Similar to section A, the SFG signal is generated by the sum of all possible photon pairs whithin the pulse bandwidth (see Fig.A1.b). As opposed to some controversial reports regarding strong enhancement for two-photon excitation of exciton resonances in TMDs [5, 6], In this case, we measure a single-photon resonant SFG process. The SFG measurements were obtained using our sub-10fs laser pulse polarized along the armchair crystallographic axis. The nonlinear response was collected using a shortpass filter and measured in our spectrometer. The SFG cumulative intensity as a function of the arctangent phase can be seen in Fig.B2.

Note C Photoluminescence Measurements

To verify we are measuring a monolayer WSe_2, we measured its Photoluminescence spectrum. The measurements were obtained using a 532nm CW diode laser.

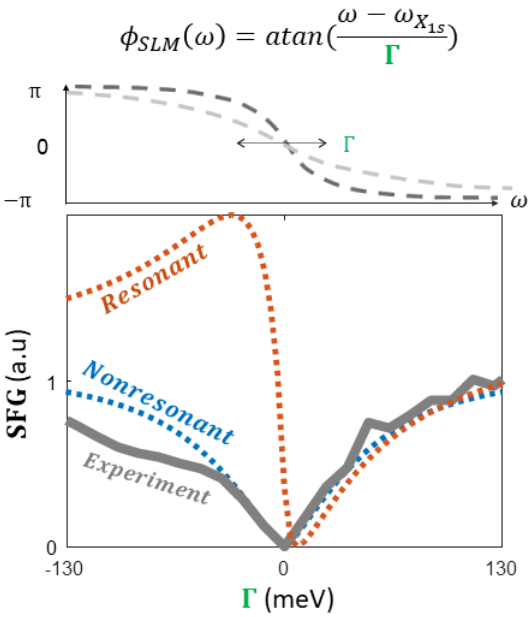

Fig. B2 Sum frequency generation (SFG) induced by different spectral phases, resonant Vs. nonresonant process. Pulse is set with an arctangent phase centered around the 1s exciton resonance, $\omega_{X_{1s}}$, and varying width Γ. We plot our experimental results (gray line) against a nonresonant SFG prediction (blue dashed line), and a resonant anharmonic oscillator (orange dashed line) which includes a quadratic displacement term.

Note D Frequency dependent 3'rd order nonlinearity

D.1 Damped Duffing Oscillator

The equation of motion of the damped Duffing oscillator $\ddot{x} + 2\gamma_0\dot{x} + \omega_0^2 x = -\frac{eE(t)}{m} - \alpha x^3$, was perturbatively solved by inserting a small perturbation to the general displacement $x(t) = x_0(t) + \delta x(t)$. Assuming $x_0(t)$ solves the linear equation of motion, we can write the solution as:

$$x_0(t) = \int \frac{e}{m}\frac{|\tilde{E}(\omega)|}{|D(\omega)|}e^{\phi_E(\omega)-\phi_D(\omega)-i\omega t}d\omega \tag{D1}$$

The equation of motion of the perturbative term $\delta x(t)$ then takes the approximate form of:

$$\delta\ddot{x}(t) + 2\gamma_0\delta\dot{x}(t) + \omega_0^2\delta x(t) \approx -\alpha x_0^3(t) \tag{D2}$$

From Eq. D2, a simple Fourier Transform will yield the result of Eq. 1 from the main text. We note that among other small terms $O(\delta x^2)$, Eq. D2 neglects the shift in resonance due to excitation. We justify this, as we have not experimentally observed any significant shift in the resonant frequency

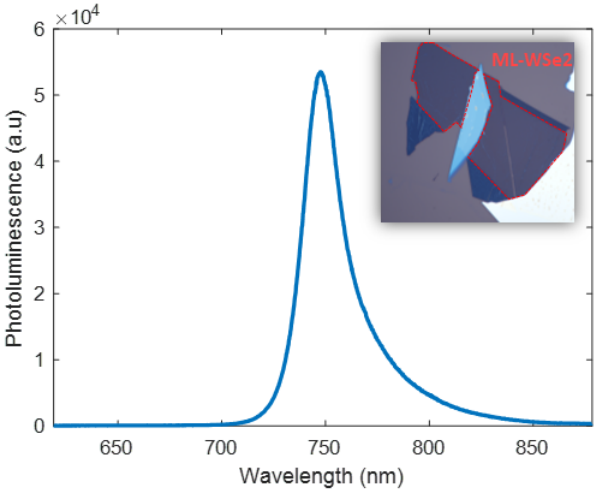

Fig. C3 Photoluminescence spectrum of a monolayer WSe_2 on $90nm$ SiO_2 on Si substrate. The measurement was obtained using a CW diode laser with wavelength $532nm$.

within the relevant range of error, and numerically, no significant difference in the resulting FWM while solving the full differential equation of motion.

D.2 Two Level System (TLS)

The TLS was modeled using the von Neumann equation [7]:

$$\dot{\hat{\rho}} = \frac{i}{\hbar}[\hat{\rho}, \hat{H}] - \gamma \begin{pmatrix} 0 & \rho_{01} \\ \rho_{10} & 0 \end{pmatrix} \tag{D3}$$

where ρ is the TLS density matrix, γ is the dephasing time associated with T_2, and $\hat{H}$ is the Hamiltonian. We note that T_1 terms can be ignored, as in room temperature T_1 for excitons in WSe2 is much larger than the dephasing time and the pulse temporal width [8–11]. The Hamiltonian of a TLS can be written as:

$$\hat{H} = \begin{pmatrix} 0 & -ea_0E(t) \\ -ea_0E(t) & \hbar\omega_0 \end{pmatrix} \tag{D4}$$

where $\hbar\omega_0$ is the energy of the excited state, e is the electron's charge, $E(t)$ is the applied electrical field and a_0 is the exciton's radius.

Taking the Fourier Transform of Eq. D3, we can then compute the off-orthogonal component ρ_{01}, which is proportional to the induced dipole moment and hence to the scattering [7, 12, 13]. While the first order gives a solution similar to the harmonic oscillator, the second order yields:

$$\delta\tilde{P}(\omega) \propto \delta\tilde{\rho}_{01}(\omega) + \delta\tilde{\rho}_{10}(\omega) \propto \frac{\tilde{E}(\omega) * ((\frac{1}{\omega}(\tilde{E}(\omega) * (\frac{\tilde{E}(\omega)(\omega+i\gamma)}{\omega^2-\omega_0^2-2i\omega\gamma}))}{\omega^2 - \omega_0^2 - 2i\omega\gamma} \tag{D5}$$

As can be seen, while proportional to E^3, the weights on the electric field are completely different than the ones in the AHO model (Eq. 1 from the main text).

References

[1] Dudovich, N., Oron, D., Silberberg, Y.: Single-pulse coherently controlled nonlinear raman spectroscopy and microscopy. Nature **418**(6897), 512–514 (2002). https://doi.org/10.1038/nature00933

[2] Ren, L., Raanan, D., Hurwitz, I., Oron, D.: High-speed low-frequency chirped coherent anti-stokes raman scattering microscopy using an ultra-steep long-pass filter. Opt. Express **27**(24), 35993–36001 (2019). https://doi.org/10.1364/OE.27.035993

[3] Min, W., Lu, S., Rueckel, M., Holtom, G.R., Xie, X.S.: Near-degenerate four-wave-mixing microscopy. Nano Lett. **9**(6), 2423–2426 (2009). https://doi.org/10.1021/nl901101g

[4] Suchowski, H., O'Brien, K., Wong, Z.J., Salandrino, A., Yin, X., Zhang, X.: Phase Mismatch–Free Nonlinear Propagation in Optical Zero-Index Materials. Science **342**(6163), 1223–1226 (2013). https://doi.org/10.1126/science.1244303. Accessed 2022-07-26

[5] Wang, G., Marie, X., Gerber, I., Amand, T., Lagarde, D., Bouet, L., Vidal, M., Balocchi, A., Urbaszek, B.: Giant enhancement of the optical second-harmonic emission of wse_2 monolayers by laser excitation at exciton resonances. Phys. Rev. Lett. **114**, 097403 (2015). https://doi.org/10.1103/PhysRevLett.114.097403

[6] Trovatello, C., Marini, A., Xu, X., Lee, C., Liu, F., Curreli, N., Manzoni, C., Dal Conte, S., Yao, K., Ciattoni, A., Hone, J., Zhu, X., Schuck, P.J., Cerullo, G.: Optical parametric amplification by monolayer transition metal dichalcogenides. Nature Photonics **15**(1), 6–10 (2021). https://doi.org/10.1038/s41566-020-00728-0

[7] Boyd, R.: Nonlinear Optics. Academic Press, San Diego, CA (2003)

[8] Steinleitner, P., Merkl, P., Nagler, P., Mornhinweg, J., Schuller, C., Korn, T., Chernikov, A., Huber, R.: Direct observation of ultrafast exciton formation in a monolayer of WSe2. Nano Letters **17**(3), 1455–1460 (2017).

https://doi.org/10.1021/acs.nanolett.6b04422

[9] Moody, G., Dass, C.K., Hao, K., Chen, C.H., Li, L.J., Singh, A., Tran, K., Clark, G., Xu, X., Berghauser, G., Malic, E., Knorr, A., Li, X.: Intrinsic homogeneous linewidth and broadening mechanisms of excitons in monolayer transition metal dichalcogenides. Nature Communications **6**(1) (2015). https://doi.org/10.1038/ncomms9315

[10] Mrejen, M., Yadgarov, L., Levanon, A., Suchowski, H.: Transient exciton-polariton dynamics in WSe 2 by ultrafast near-field imaging. Science Advances **5**(2) (2019). https://doi.org/10.1126/sciadv.aat9618

[11] Merkl, P., Mooshammer, F., Brem, S., Girnghuber, A., Lin, K.Q., Weigl, L., Liebich, M., Yong, C.K., Gillen, R., Maultzsch, J., Lupton, J.M., Malic, E., Huber, R.: Twist-tailoring coulomb correlations in van der waals homobilayers. Nature Communications **11**(1) (2020). https://doi.org/10.1038/s41467-020-16069-z

[12] Fotso, H.F., Dobrovitski, V.V.: Absorption spectrum of a two-level system subjected to a periodic pulse sequence. Physical Review B **95**(21) (2017). https://doi.org/10.1103/physrevb.95.214301

[13] Mollow, B.R.: Power spectrum of light scattered by two-level systems. Physical Review **188**(5), 1969–1975 (1969). https://doi.org/10.1103/physrev.188.1969